

# Glassy gels toughened by solvent

<https://doi.org/10.1038/s41586-024-07564-0>

Received: 2 June 2023

Accepted: 14 May 2024

Published online: 19 June 2024

 Check for updates

Meixiang Wang<sup>1,6</sup>, Xun Xiao<sup>2,6</sup>, Salma Siddika<sup>3</sup>, Mohammad Shamsi<sup>1</sup>, Ethan Frey<sup>1</sup>, Wen Qian<sup>4</sup>, Wubin Bai<sup>2</sup>, Brendan T. O'Connor<sup>5</sup> & Michael D. Dickey<sup>1,✉</sup>

Glassy polymers are generally stiff and strong yet have limited extensibility<sup>1</sup>. By swelling with solvent, glassy polymers can become gels that are soft and weak yet have enhanced extensibility<sup>1–3</sup>. The marked changes in properties arise from the solvent increasing free volume between chains while weakening polymer–polymer interactions. Here we show that solvating polar polymers with ionic liquids (that is, ionogels<sup>4,5</sup>) at appropriate concentrations can produce a unique class of materials called glassy gels with desirable properties of both glasses and gels. The ionic liquid increases free volume and therefore extensibility despite the absence of conventional solvent (for example, water). Yet, the ionic liquid forms strong and abundant non-covalent crosslinks between polymer chains to render a stiff, tough, glassy, and homogeneous network (that is, no phase separation)<sup>6</sup>, at room temperature. Despite being more than 54 wt% liquid, the glassy gels exhibit enormous fracture strength (42 MPa), toughness (110 MJ m<sup>-3</sup>), yield strength (73 MPa) and Young's modulus (1 GPa). These values are similar to those of thermoplastics such as polyethylene, yet unlike thermoplastics, the glassy gels can be deformed up to 670% strain with full and rapid recovery on heating. These transparent materials form by a one-step polymerization and have impressive adhesive, self-healing and shape-memory properties.

The mechanical properties of glassy polymers are important for many consumer products<sup>1,7</sup>. Owing to the strong interactions between polymer chains, glassy polymers are stiff (around 1 GPa modulus) and strong (10–100 MPa fracture strength)<sup>1</sup>. Solvating a glassy polymer renders it a gel. For example, contact lenses are polymeric gels swollen with water. The solvent in a gel decreases polymer–polymer interactions and softens the polymer network, thereby diminishing the mechanical properties<sup>8,9</sup>. Gels typically have a modulus of 0.0001 GPa and fracture strength <1 MPa<sup>2,3</sup>. Yet, the high loading of solvent and, thus, increased free volume (that is, volume not occupied by polymer) found in gels can provide benefits: increasing the stretchability of polymer networks by one to two orders of magnitude relative to glassy polymers while providing additional functionality, such as serving as an electrolyte<sup>4,10</sup>. Thus, glassy polymers and gels have distinct trade-offs: glassy systems are dry, stiff and strong, whereas gels are solvated, soft and weak. Furthermore, glassy polymers typically undergo brittle failure or plastic deformation at low strains, whereas gels can extend elastically, often to high strains.

Strategies to toughen gels generally focus on promoting or mediating polymer–polymer interactions, including (1) secondary bonds between polymer chains to dissipate energy during deformation<sup>2,6,11</sup>; and (2) polymer entanglements or fillers to help distribute stress in a gel network<sup>12–14</sup>. Despite occupying a large portion (>50 wt%) of gels, solvents are effectively ignored or even regarded as detrimental to stiffening or toughening because they lessen polymer–polymer interactions. In principle, if a solvent could interact strongly between polymer chains, it could have the benefits of a solvent (for example, extensibility), but without compromising stiffness or strength.

Here we report homogeneous glassy gels toughened and vitrified by solvents. The solvent–ionic liquid imparts gel-like extensibility to the polymer similar to a conventional solvent. Yet, at optimized ionic liquid concentrations, the ionic liquid forms abundant and strong non-covalent interactions with the polymer chains (that is, 'solvent crosslinking') to impart glassy properties (Fig. 1a). As a result, these glassy gels possess modulus and strength similar to glassy polymers yet maintain gel-like elongation and recovery (Extended Data Fig. 1). Combined, these properties result in substantial toughness, similar to that of common thermoplastics such as polyethylene (PE). Herein, we use the term 'toughness' to refer to the area under a stress–strain curve, although it could also be called fracture energy. Tough ionogels have been prepared previously using phase separation to promote polymer–polymer interactions in a heterogeneous network<sup>6</sup>. By contrast, glassy gels—which are an order of magnitude stiffer and tougher—achieve toughness by solvent crosslinking the polymer in a homogeneous network. The solvent crosslinks are useful for self-healing and shape memory, whereas the use of ionic liquid gives the glassy gel notable thermal stability and remarkable adhesive properties.

Notably, the glassy gels form in a single step by photopolymerization at room temperature. Yet, many polymers with similar mechanical properties, such as PE, are not readily compatible with photopolymerization and thus require two separate steps: synthesis in a chemical plant using catalysts followed by melt processing at highly elevated temperatures and/or pressures, such as injection moulding. Moreover, glassy gels can be formed using a variety of ionic liquids and monomers. Thus, these findings provide a simple and versatile route to make polymeric parts or coatings on demand with attractive properties of gels (high solvation

<sup>1</sup>Department of Chemical and Biomolecular Engineering, North Carolina State University, Raleigh, NC, USA. <sup>2</sup>Department of Applied Physical Sciences, University of North Carolina, Chapel Hill, NC, USA. <sup>3</sup>Department of Materials Science and Engineering and Organic and Carbon Electronic Laboratories (ORaCEL), North Carolina State University, Raleigh, NC, USA. <sup>4</sup>Department of Mechanical and Materials Engineering, University of Nebraska–Lincoln, Lincoln, NE, USA. <sup>5</sup>Department of Mechanical and Aerospace Engineering and Organic and Carbon Electronic Laboratories (ORaCEL), North Carolina State University, Raleigh, NC, USA. <sup>6</sup>These authors contributed equally: Meixiang Wang, Xun Xiao. ✉e-mail: mddickey@ncsu.edu

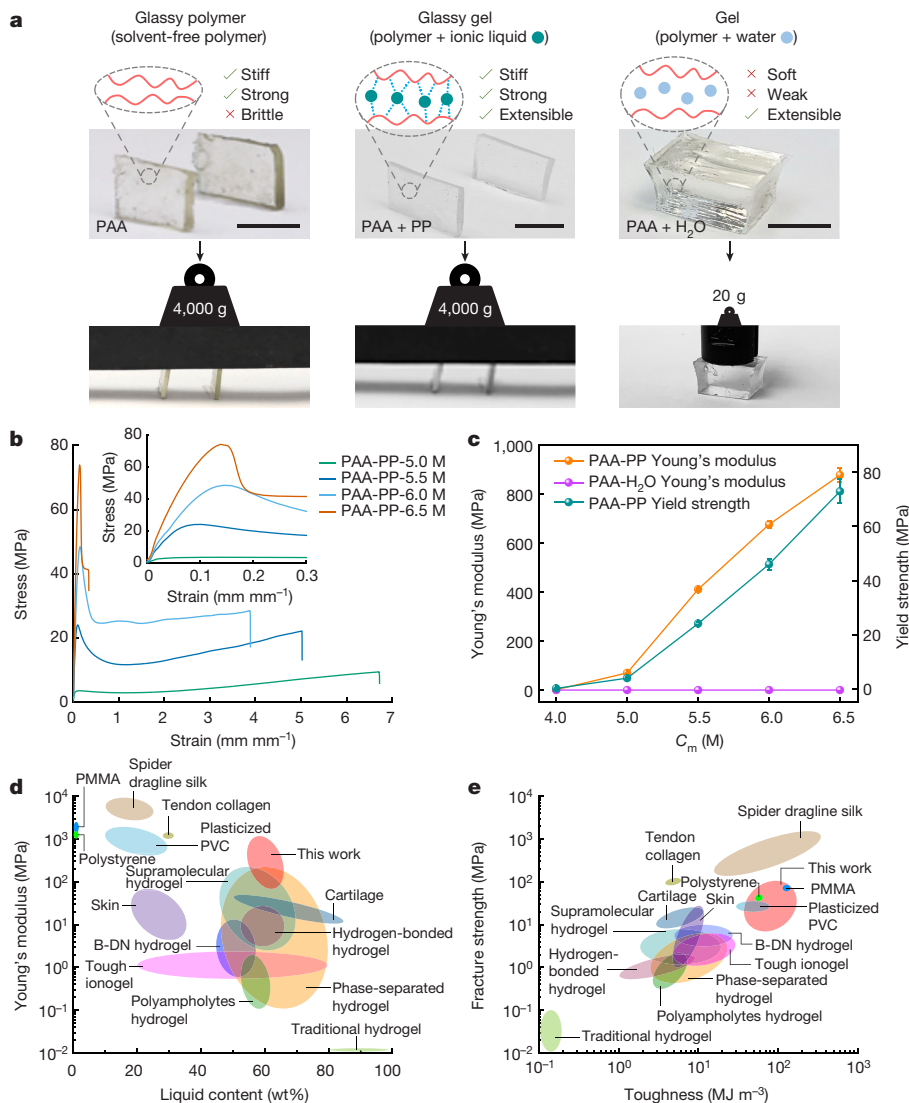


**Fig. 1 | Mechanical properties of glassy gels.** **a**, The glassy polymer (here, poly(acrylic acid), PAA) is solvent-free, stiff and strong, but brittle. The glassy gel (that is, PAA solvated by ionic liquid, PP) is physically crosslinked by the ionic liquid solvent and becomes stiff, strong and extensible, whereas the gel (that is, PAA solvated by water) lacks solvent crosslinking and becomes soft and weak, but extensible. As a result, the glassy polymer and glassy gel can hold 4,000 g, whereas the gel can only hold up to 20 g despite being about seven times wider. The scale bar is 10 mm. **b**, Tensile stress–strain behaviour is highly

composition dependent (inset, the magnification of **b**). **c**, Summary of Young's modulus and yield strength of gels with different concentrations of AA monomer, C<sub>m</sub>. **d,e**, Comparison of this work and various gels, glassy and plasticized polymers, biological tissues such as skin, cartilage, tendon collagen and spider dragline silk in terms of Young's modulus and liquid content (**d**) and fracture strength and toughness (**e**). B-DN, block double-network. Error bars on the data show standard deviation from three independent samples.

and large elongation), glasses (stiffness and strength), thermoplastics (toughness), crosslinked networks (strain recovery) and ionic liquids (nonvolatility and conductivity).

### Synthesis and properties of glassy gels

The glassy gel forms by one-step photopolymerization of a solution containing monomer (acrylic acid, AA), crosslinker (*N,N'*-methylenebis(acrylamide), MBAA), photoinitiator (Irgacure 2959, I2959) and ionic liquid (tributyl(methyl)phosphonium dimethyl phosphate, PP) (Extended Data Fig. 2a, Supplementary Fig. 1 and Supplementary Video 1). We fabricated a series of gels with the nomenclature *PM-S-C<sub>m</sub>*, where *M*, *S* and *C<sub>m</sub>* are the monomer, solvent and molar concentration of monomer, respectively. P stands for 'poly' as in polymer. For example, PAA-PP-4.0 M gel is prepared by polymerizing 4.0 M AA in PP solvent. The polymerization proceeded to high apparent conversion (>94%; Supplementary Fig. 2a). The resulting gels have a

high liquid content (>54 wt%) and are highly transparent, similar to PAA-H<sub>2</sub>O, a common conventional hydrogel (Extended Data Fig. 2b and Supplementary Fig. 2b). Yet, compared with PAA-H<sub>2</sub>O, the resulting glassy gels exhibit stable weight and mechanical properties because of the low volatility of PP relative to H<sub>2</sub>O (Extended Data Fig. 2c and Supplementary Fig. 2c–f).

The tensile properties of PAA-PP gels are remarkable considering they are highly solvated (Fig. 1b). Depending on the concentration of AA, the gels can vary from being either stiff and brittle, stiff and tough, or soft and stretchable (Supplementary Fig. 3). For example, when C<sub>m</sub> is 4.0 M, the PAA-PP gel is stretchable and soft, as expected for a highly solvated gel (Supplementary Fig. 3d,e). However, as C<sub>m</sub> increases, the Young's modulus and yield strength increase by nearly three orders of magnitude, reaching a maximum modulus of about 1 GPa, yield strength of 73 MPa, and toughness of 110 MJ m<sup>-3</sup> depending on the composition (Fig. 1c and Supplementary Table 1). The glassy gels can support at least 2.6 × 10<sup>4</sup> times their own weight

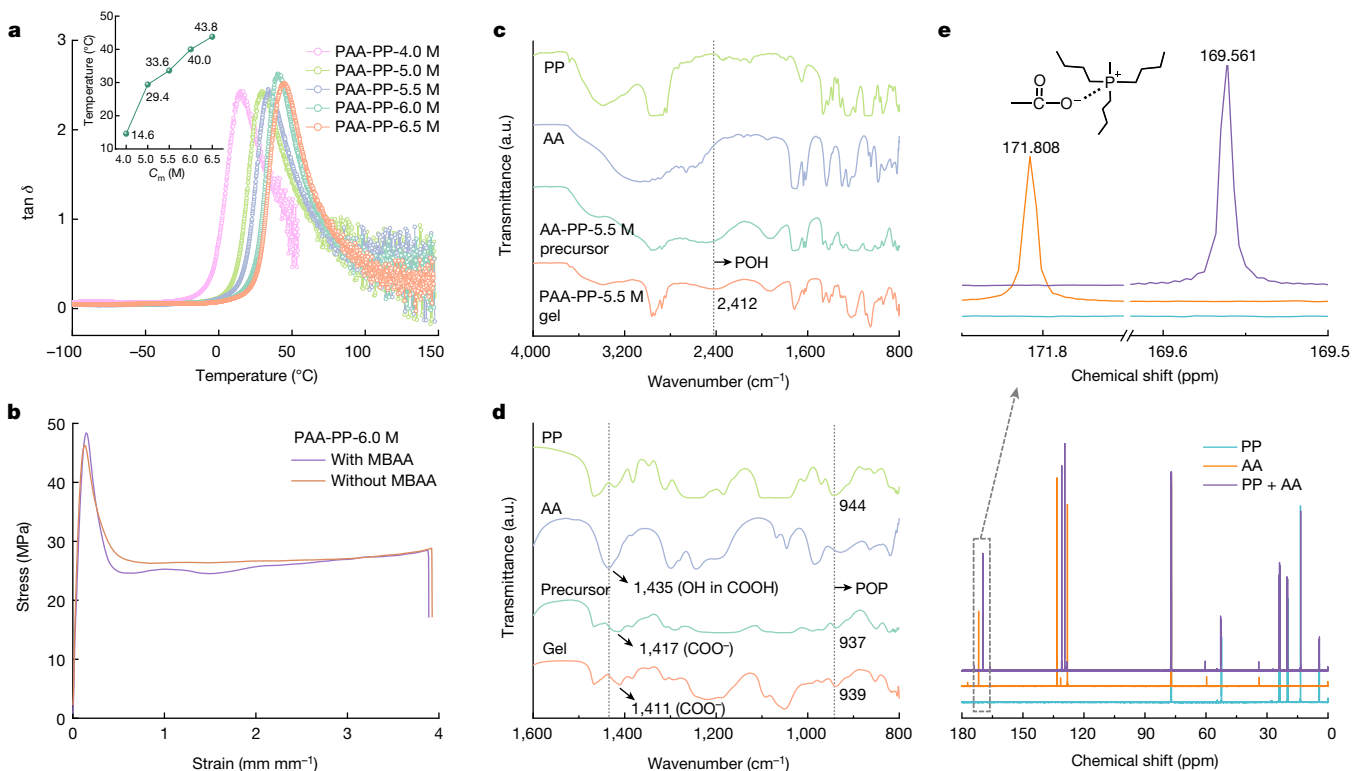


**Fig. 2 | Characterization of PAA-PP gels.** **a**, Temperature dependence of the loss tangent ( $\tan \delta$ ). Inset, the  $T_g$  (measured from the peak of  $\tan \delta$ ) of different gels. **b**, Tensile stress–strain curves of glassy gels with and without MBAA, the covalent crosslinker. **c**, FTIR of various materials. **d**, Magnification of c

(800–1,600  $\text{cm}^{-1}$ ). The transmittance in **c** and **d** is normalized. **e**,  $^{13}\text{C}$  NMR spectra of PP solvent, AA monomer and their mixture ( $C_m = 6.0$  M). The magnified  $^{13}\text{C}$  NMR spectra of carbon in the carboxyl group of AA is shown at the top. Taken in sum, these results show strong solvent (PP) and monomer (AA) interactions.

(Supplementary Video 2). By contrast, PAA- $\text{H}_2\text{O}$  hydrogels are weak and their Young's modulus (0.07–0.18 MPa) changes negligibly over the same  $C_m$  (Fig. 1c and Supplementary Fig. 4).

Figure 1d,e and Supplementary Table 2 show that the Young's modulus, fracture strength and toughness of PAA-PP gels far exceed those of skin, cartilage and most synthetic gels<sup>3,15–27</sup>. Although most of the gel is liquid (>54 wt%), the mechanical properties of PAA-PP glassy gels are still comparable to or better than those of glassy polymers (for example, polymethylmethacrylate (PMMA) and polystyrene), plasticized polyvinyl chloride (PVC, <30 wt% plasticizer), and spider dragline silk (an ultra-tough natural fibre containing around 20 wt% liquid)<sup>28–34</sup>. Furthermore, the stress–strain behaviour of PAA-PP glassy gels is similar to that of many thermoplastics such as PE that cannot be photopolymerized<sup>35</sup>. Notably, glassy polymers (and, more broadly, thermoplastics) undergo brittle failure or permanent plastic deformation in response to strain, whereas PAA-PP glassy gels can recover fully and rapidly (<1 min at 80 °C; Supplementary Fig. 5 and Supplementary Video 3).

### Characterization and toughening mechanism

The distinct difference in mechanical behaviours of PAA-PP and PAA- $\text{H}_2\text{O}$  gels suggests that the solvent plays an important part in toughening. For example, PAA- $\text{H}_2\text{O}$ -6.0 M has a Young's modulus approximately 10,000 times smaller than the PAA-PP-6.0 M gel (Supplementary Fig. 4). The differences cannot be attributed to toughening via phase separation<sup>6</sup>, because the PAA-PP gels show a homogeneous morphology under scanning electron microscopy while having a single glass transition temperature ( $T_g$ ; Fig. 2a and Supplementary Fig. 6a).

The tensile properties of the glassy gels are nearly identical at 0 mol% and 0.1 mol% MBAA crosslinker, which indicates that covalent crosslinking is not responsible for the enormous stiffness in the glassy gels

(Fig. 2b). To avoid decreasing extensibility (Supplementary Fig. 6b–i), the MBAA concentration is fixed at 0.1 mol% in which its only notable role is to enable full strain recovery.

Strong solvent–polymer interactions can be inferred from the exothermic mixing (Supplementary Fig. 7a,b and Supplementary Video 4) and by the presence of a  $T_g$  above room temperature at  $C_m > 4.0$  M despite the free volume provided by the ionic liquid (Fig. 2a, inset). Fourier transform infrared (FTIR) spectroscopy helps identify the nature of these interactions (Fig. 2c,d). Using  $C_m = 5.5$  M as an example, the in-plane bending vibration of OH in the carboxyl group (COOH) of AA at 1,435  $\text{cm}^{-1}$  red shifts to 1,417  $\text{cm}^{-1}$  and 1,411  $\text{cm}^{-1}$  in the precursor solution and glassy gel, respectively<sup>36,37</sup> (Fig. 2d). This shift is consistent with COOH dissociating to form  $\text{COO}^-$  and  $\text{H}^+$  in PP. Moreover, a peak at 2,412  $\text{cm}^{-1}$  occurs in the spectra of both the precursor solution and the glassy gel that is absent in the spectra of both pure PP and pure AA (Fig. 2c). This peak is assigned to POH, which suggests an interaction between the ionic liquid anion ( $\text{PO}^-$ ) and the  $\text{H}^+$  cation dissociated from AA<sup>38</sup>. Notably, the peak at 944  $\text{cm}^{-1}$  in the PP spectrum corresponds to the POP vibration of the  $\text{PO}^-$  anion and  $\text{P}^+$  cation shifted to 937  $\text{cm}^{-1}$  in the precursor solution and 939  $\text{cm}^{-1}$  in the glassy gel<sup>39</sup>. This may be ascribed to the altered cation–anion interactions in PP arising from the new interactions between PP and AA on mixing. The interaction between PP and AA is also evidenced by the  $^{13}\text{C}$  NMR spectra (Fig. 2e). A large chemical shift of carbon in the carboxyl group is observed because of the electrostatic interactions between  $\text{COO}^-$  and  $\text{P}^+$ . Collectively, these results indicate that the ionic liquid anion ( $\text{PO}^-$ ) interacts with the dissociated  $\text{H}^+$  and the ionic liquid cation ( $\text{P}^+$ ) interacts with  $\text{COO}^-$  of the polymer (Supplementary Fig. 7c). Apart from electrostatic interactions, hydrogen bonds may also form between the anion of ionic liquid and non-dissociated PAA to promote their compatibility<sup>40</sup>. As further evidence of strong binding facilitated by the solvent, PAA-PP-6.0 M barely swells when

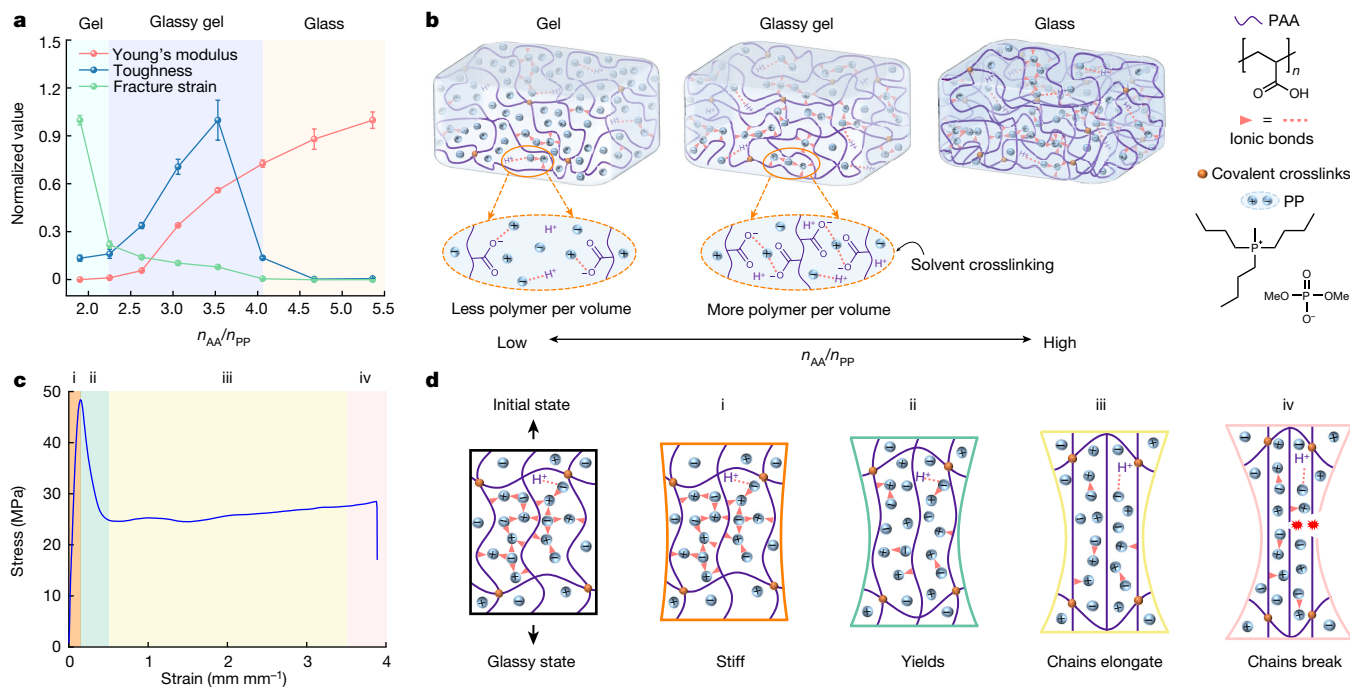


**Fig. 3 | Toughening mechanism of PAA-PP gels.** **a**, Normalized Young's modulus, fracture strain and toughness of glassy gels as a function of the molar ratio of monomer (AA) to ionic liquid solvent (PP),  $n_{AA}/n_{PP}$ . As the molar ratio changes, the mechanical behaviour of the gels varies from soft and stretchable (gel-like), stiff and tough (glassy gel), to stiff and brittle (glass-like). **b**, When  $n_{AA}/n_{PP}$  is low, the chains are separated by excess solvent, resulting in a soft gel. As the molar ratio increases, more solvent crosslinks form between the chains,

resulting in a glassy gel. Further increasing  $n_{AA}/n_{PP}$  results in sufficient crosslinks to form a stiff network, but insufficient solvent to give extensibility; thus, a brittle glass. **c**, The tensile stress-strain curve of a glassy gel, PAA-PP-6.0 M, is divided into four regimes (i-iv). **d**, The deformation mechanism of the glassy gel during elongation. Error bars on the data show standard deviation from three independent samples.

submerged in ionic liquid for 7 days, whereas PAA-H<sub>2</sub>O-6.0 M gel swells markedly in water (Supplementary Fig. 8). These results are consistent with the presence of strong non-covalent crosslinking of the glassy gel, which seems to originate from the interaction of ions in the ionic liquid (that is, P<sup>+</sup> cation and PO<sup>-</sup> anion) and the interaction of ionic liquid and polymer (for example, P<sup>+</sup> cation and COO<sup>-</sup>) discussed above.

In sum, the results indicate a solvent toughening mechanism for the glassy gel (Fig. 3). The ions in the solvent act as crosslinkers that bridge the polymer chains by strong electrostatic interactions. The molar ratio of monomer (AA) to solvent (PP),  $n_{AA}/n_{PP}$ , controls the mechanical behaviour of the gels from soft and stretchable, stiff and tough, to stiff and brittle (Fig. 3a, Supplementary Fig. 3 and Supplementary Table 1). At a low molar ratio ( $n_{AA}/n_{PP} < 2.25$ , that is,  $C_m < 4.5$  M), the number of polymer chains per volume is low. Thus, there are few electrostatic crosslinks between chains, resulting in a gel that is soft and highly extensible with a low  $T_g$  (for example, 14.6 °C for 4.0 M, Fig. 3b). When the molar ratio increases ( $2.25 \leq n_{AA}/n_{PP} < 4.06$ , that is,  $4.5 \text{ M} \leq C_m < 6.5 \text{ M}$ ), the number of polymer chains per volume increases, whereas the distance between the chains decreases. This enables more direct electrostatic interactions to physically crosslink the chains, forming a glassy gel that enables gel-like stretchability and thermoplastic-like stiffness (Fig. 3b). The cation diameter of PP is about three times the length of a polymerized AA repeat unit, which may explain the magnitude of these ratios. Increasing  $n_{AA}/n_{PP} \geq 4.06$  ( $C_m \geq 6.5$  M) further shortens the interchain distance allowing solvent-mediated crosslinks, yet insufficient solvent to provide extensibility, resulting in a glass-like network with high yield and fracture strength, but brittle failure (Fig. 3b).

Figure 3c,d shows the mechanical behaviours of the glassy gels during elongation. Taking PAA-PP-6.0 M gel as an example, the stress-strain curve is divided into four regimes (Fig. 3c,d). At low strain (regime i), the

network is elastic with a huge Young's modulus (that is, slope) because of the strong non-covalent interactions. In regime ii, the network of non-covalent interactions yields, the chains start to elongate and the stress drops. In regime iii, the samples form a stable neck and undergo a cold-drawing process to their tensile limit. As a result, the stress almost plateaus (about 26 MPa), whereas the strain increases markedly from 50% to 350%. In regime iv, covalent bonds in the polymer network break and the glassy gel fails.

### Generalized strategy for synthesizing glassy gels

Solvent crosslinking occurs with other polymers and ionic liquids. We synthesized PAA gels with three different ionic liquids: tributyl(methyl) phosphonium methyl sulfate (PS), 1-ethyl-3-methylimidazolium dimethyl phosphate (NP), and 1-ethyl-3-methylimidazolium ethyl sulfate (NS) (Supplementary Fig. 1). These ionic liquids were chosen based on the rationale that PS has the same cation as PP, NP has the same anion as PP and NS has nearly the same cation or anion as NP or PS (but is distinct from PP). All three ionic liquids formed homogeneous PAA glassy gels with a single  $T_g$  and a <sup>13</sup>C NMR chemical shift of carbon in the carboxyl group, similar to PAA-PP gels (Supplementary Fig. 9). Moreover, these PAA glassy gels showed thermoplastic-like modulus (about 1 GPa), yield strength (>35 MPa) and a gel-like elongation (>300% strain) (Fig. 4a). Similar to PAA-PP, the networks formed using PS, NP and NS had mechanical properties dependent on molar ratio (Fig. 4b, Supplementary Fig. 10-12 and Supplementary Tables 3-5). The mechanical properties of the glassy gels can also be greatly tuned by mixing different ionic liquids to control their interactions with the polymer chains and thus the solvent crosslinking (Supplementary Fig. 13).

The solvent crosslinking strategy in Figs. 1-3 is achieved through ion-ion interactions by dissociated AA monomer. Yet, ion-dipole

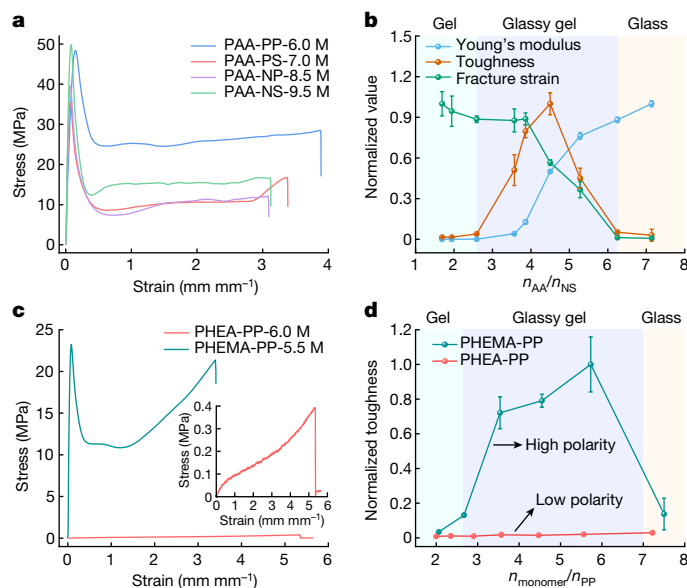


**Fig. 4 | Generalized strategy for glassy gels.** **a**, Tensile stress–strain curves of PAA gels with different ionic liquids are all tough and glassy. **b**, Normalized Young’s modulus, toughness and fracture strain of PAA-NS gels as a function of the molar ratio of AA to NS ( $n_{AA}/n_{NS}$ ). **c**, Tensile stress–strain curves of PHEA-PP-6.0 M and PHEMA-PP-5.5 M gels. Inset, magnification of the tensile curve of PHEA-PP-6.0 M gel. **d**, Normalized toughness of PHEA-PP and PHEMA-PP gels as a function of the molar ratio of monomer to PP ( $n_{monomer}/n_{PP}$ ). High polarity and low polarity refer to the polarity of PHEMA and PHEA polymers in the gels, respectively. To make a clear comparison, both PHEA-PP and PHEMA-PP gels are normalized based on the maximum toughness of PHEMA-PP gels. In **b** and **d**, the mechanical behaviour of all the materials except PHEA-PP vary from soft and stretchable (gel-like), stiff and tough (glassy gel), to stiff and brittle (glass-like) as the molar ratio changes. Error bars on the data show standard deviation from three independent samples.

interactions can also be applied to toughen polymers that cannot dissociate. Two monomers, 2-hydroxyethyl acrylate (HEA) and 2-hydroxyethyl methacrylate (HEMA), which do not dissociate as readily as AA, were studied (Supplementary Fig. 1). Both produce homogeneous gels with a single phase (Supplementary Fig. 14). Yet, the Young’s modulus (560 MPa) and fracture strength (21 MPa) of PHEMA-PP-5.5 M far exceed those of PHEA-PP-6.0 M (Young’s modulus of 0.25 MPa, fracture strength of 0.4 MPa), with a similar molar ratio of monomer to ionic liquid (Fig. 4c). Note that the PHEA-PP networks remain soft at all concentrations studied, whereas the PHEMA-PP networks are markedly toughened and show glassy behaviours at molar ratios above 2.67 (Fig. 4d, Supplementary Fig. 15 and Supplementary Tables 6 and 7). The distinct mechanical properties of PHEA-PP and PHEMA-PP likely originate from the polarity difference, which has been further verified by studying other monomers (Supplementary Figs. 16 and 17 and Supplementary Note 1).

In sum, the formation of glassy gel requires (1) solvent interacting strongly with polymer chains to form physical crosslinking, in which the interaction strength can be tuned by modifying the polarity of the monomers and varying the ions in the ionic liquid solvent; (2) an appropriate molar ratio of monomer to ionic liquid (that is,  $n_{monomer}/n_{ionic\ liquid}$ ) to optimize the density of solvent crosslinks without compromising extensibility. At lower ratios of monomer to ionic liquid (that is, higher solvent content), the ionic liquids plasticize the polymer to form a gel by moving the polymer chains further apart, whereas too little solvent does not give the polymer extensibility (that is, brittle glass). In the materials studied here, the optimal molar ratio is about 3–5. The exact value should depend on the molecular sizes and interaction strength between the monomer and the ions.

## Functionality and application

Apart from the outstanding mechanical properties, solvent crosslinking also endows the glassy gel with several functions, including exceptional adhesive properties, shape memory and self-healing (Extended Data Fig. 3, Supplementary Fig. 18 and Supplementary Videos 5–7), which have been discussed in Supplementary Note 2. The remarkable thermal stability of ionic liquid enables the glassy gel to be used as Joule heat-driven grippers (Supplementary Fig. 19, Supplementary Video 8 and Supplementary Note 3), whereas the modest conductivity of ionic liquid differentiates these materials from most glassy polymers (Supplementary Fig. 20). Thus, these materials could find applications in electronics, batteries and sensors.

## Summary

We report a glassy gel with high solvent loading using a facile one-step process, during which the gel is toughened in situ by solvent. The solvent forms abundant, strong, yet non-covalent crosslinks with polymer chains. Generally, highly solvated polymers form gels that are soft, weak and extensible. By contrast, the homogeneous glassy gels reported here have a modulus and strength similar to those of thermoplastics, yet retain the ability to reach large strains and full strain recovery similar to a highly solvated gel. These remarkable mechanical properties arise from abundant electrostatic interactions (for example, ion–ion or ion–dipole interactions) between the ionic liquid solvent and polymer chains, which place the network in a glassy state at room temperature, enable extensibility and dissipate the energy during deformation. Therefore, despite being highly solvated, the glassy gels have a  $T_g$  above room temperature, enabling shape memory and self-healing. Although the glassy gels are glassy and stiff, the solvent gives them remarkable adhesive properties because of the ability to form strong interactions with interfaces. The glassy gels can become more glass-like or gel-like depending on the ratio and selection of monomer and solvent, as well as temperature. Glassy gels form simply by photopolymerization, yet have mechanical properties similar to common plastics such as those of PE that require laborious synthesis and melt processing. These findings provide a simple route to create a new class of materials featuring attractive properties of glassy polymers, thermoplastics and gels formed with the ease of photopolymerization.

## Online content

Any methods, additional references, Nature Portfolio reporting summaries, source data, extended data, supplementary information, acknowledgements, peer review information; details of author contributions and competing interests; and statements of data and code availability are available at <https://doi.org/10.1038/s41586-024-07564-0>.

- Young, R. J. & Lovell, P. A. *Introduction to Polymers* (CRC Press, 2011).
- Sun, J.-Y. et al. Highly stretchable and tough hydrogels. *Nature* **489**, 133–136 (2012).
- Sun, T. L. et al. Physical hydrogels composed of polyampholytes demonstrate high toughness and viscoelasticity. *Nat. Mater.* **12**, 932–937 (2013).
- Wang, M., Hu, J. & Dickey, M. D. Tough ionogels: synthesis, toughening mechanisms, and mechanical properties—a perspective. *JACS Au* **2**, 2645–2657 (2022).
- Wang, M., Hu, J. & Dickey, M. D. Emerging applications of tough ionogels. *NPG Asia Mater.* **15**, 66 (2023).
- Wang, M. et al. Tough and stretchable ionogels by in situ phase separation. *Nat. Mater.* **21**, 359–365 (2022).
- Geyer, R., Jambeck, J. R. & Law, K. L. Production, use, and fate of all plastics ever made. *Sci. Adv.* **3**, e1700782 (2017).
- Fan, H. & Gong, J. P. Fabrication of bioinspired hydrogels: challenges and opportunities. *Macromolecules* **53**, 2769–2782 (2020).
- Ueki, T. & Watanabe, M. Polymers in ionic liquids: dawn of neoteric solvents and innovative materials. *Bull. Chem. Soc. Jpn* **85**, 33–50 (2012).
- Liu, X., Liu, J., Lin, S. & Zhao, X. Hydrogel machines. *Mater. Today* **36**, 102–124 (2020).
- Gong, J. P., Katsuyama, Y., Kurokawa, T. & Osada, Y. Double-network hydrogels with extremely high mechanical strength. *Adv. Mater.* **15**, 1155–1158 (2003).
- Zhao, X. Multi-scale multi-mechanism design of tough hydrogels: building dissipation into stretchy networks. *Soft Matter* **10**, 672–687 (2014).

13. Kim, J., Zhang, G., Shi, M. & Suo, Z. Fracture, fatigue, and friction of polymers in which entanglements greatly outnumber cross-links. *Science* **374**, 212–216 (2021).
14. Kamiyama, Y. et al. Highly stretchable and self-healable polymer gels from physical entanglements of ultrahigh-molecular weight polymers. *Sci. Adv.* **8**, eadd0226 (2022).
15. Gong, J. P. Why are double network hydrogels so tough? *Soft Matter* **6**, 2583–2590 (2010).
16. Corkhill, P. H., Trevett, A. S. & Tighe, B. J. The potential of hydrogels as synthetic articular cartilage. *Proc. Inst. Mech. Eng. H* **204**, 147–155 (1990).
17. Cao, Z., Liu, H. & Jiang, L. Transparent, mechanically robust, and ultrastable ionogels enabled by hydrogen bonding between elastomers and ionic liquids. *Mater. Horiz.* **7**, 912–918 (2020).
18. Yu, L. et al. Highly tough, Li-metal compatible organic–inorganic double-network solvate ionogel. *Adv. Energy Mater.* **9**, 1900257 (2019).
19. Ren, Y. et al. Ionic liquid–based click-ionogels. *Sci. Adv.* **5**, eaax0648 (2019).
20. Gallagher, A. J. et al. Dynamic tensile properties of human skin. In *2012 IRCOBI Conference Proc.* 494–502 (International Research Council on the Biomechanics of Injury, 2012).
21. Sato, K. et al. Phase-separation-induced anomalous stiffening, toughening, and self-healing of polyacrylamide gels. *Adv. Mater.* **27**, 6990–6998 (2015).
22. Zhang, H. J. et al. Tough physical double-network hydrogels based on amphiphilic triblock copolymers. *Adv. Mater.* **28**, 4884–4890 (2016).
23. Joodaki, H. & Panzer, M. B. Skin mechanical properties and modeling: a review. *Proc. Inst. Mech. Eng. H* **232**, 323–343 (2018).
24. Wang, Y. J. et al. Ultrastiff and tough supramolecular hydrogels with a dense and robust hydrogen bond network. *Chem. Mater.* **31**, 1430–1440 (2019).
25. Weng, D. et al. Polymeric complex-based transparent and healable ionogels with high mechanical strength and ionic conductivity as reliable strain sensors. *ACS Appl. Mater. Interfaces* **12**, 57477–57485 (2020).
26. Zhang, X., Du, C., Du, M., Zheng, Q. & Wu, Z. L. Kinetic insights into glassy hydrogels with hydrogen bond complexes as the cross-links. *Mater. Today Phys.* **15**, 100230 (2020).
27. Hu, X., Vatankehah-Varnoosfaderani, M., Zhou, J., Li, Q. & Sheiko, S. S. Weak hydrogen bonding enables hard, strong, tough, and elastic hydrogels. *Adv. Mater.* **27**, 6899–6905 (2015).
28. Yarger, J. L., Cherry, B. R. & van Der Vaart, A. Uncovering the structure–function relationship in spider silk. *Nat. Rev. Mater.* **3**, 18008 (2018).
29. Guo, Y. et al. Enhancing impact resistance of polymer blends via self-assembled nanoscale interfacial structures. *Macromolecules* **51**, 3897–3910 (2018).
30. Liu, J. et al. Polystyrene glasses under compression: ductile and brittle responses. *ACS Macro Lett.* **4**, 1072–1076 (2015).
31. Zhu, H. et al. Biobased plasticizers from tartaric acid: synthesis and effect of alkyl chain length on the properties of poly(vinyl chloride). *ACS Omega* **6**, 13161–13169 (2021).
32. Pita, V. J. R. R., Sampaio, E. E. M. & Monteiro, E. E. C. Mechanical properties evaluation of PVC/plasticizers and PVC/thermoplastic polyurethane blends from extrusion processing. *Polym. Test.* **21**, 545–550 (2002).
33. Huang, Q., Wan, C., Loveridge, M. & Bhagat, R. Partially neutralized polyacrylic acid/poly(vinyl alcohol) blends as effective binders for high-performance silicon anodes in lithium-ion batteries. *ACS Appl. Energy Mater.* **1**, 6890–6898 (2018).
34. Eisenberg, A., Yokoyama, T. & Sambalido, E. Dehydration kinetics and glass transition of poly(acrylic acid). *J. Polym. Sci.* **7**, 1717–1728 (1969).
35. Song, P. A., Yu, Y., Wu, Q. & Fu, S. Facile fabrication of HDPE-g-MA/nanodiamond nanocomposites via one-step reactive blending. *Nanoscale Res. Lett.* **7**, 355 (2012).
36. Max, J.-J. & Chapados, C. Infrared spectroscopy of aqueous carboxylic acids: comparison between different acids and their salts. *J. Phys. Chem. A* **108**, 3324–3337 (2004).
37. Parikh, S. J., Mukome, F. N. D. & Zhang, X. ATR-FTIR spectroscopic evidence for biomolecular phosphorus and carboxyl groups facilitating bacterial adhesion to iron oxides. *Colloids Surf. B Biointerfaces* **119**, 38–46 (2014).
38. Rungrodnimitchai, S. Rapid preparation of biosorbents with high ion exchange capacity from rice straw and bagasse for removal of heavy metals. *Sci. World J.* **2014**, 634837 (2014).
39. Qu, J. et al. Synergistic effects between phosphonium-alkylphosphate ionic liquids and zinc dialkyldithiophosphate (ZDDP) as lubricant additives. *Adv. Mater.* **27**, 4767–4774 (2015).
40. Swatloski, R. P., Spear, S. K., Holbrey, J. D. & Rogers, R. D. Dissolution of cellulose with ionic liquids. *J. Am. Chem. Soc.* **124**, 4974–4975 (2002).

**Publisher's note** Springer Nature remains neutral with regard to jurisdictional claims in published maps and institutional affiliations.

Springer Nature or its licensor (e.g. a society or other partner) holds exclusive rights to this article under a publishing agreement with the author(s) or other rightsholder(s); author self-archiving of the accepted manuscript version of this article is solely governed by the terms of such publishing agreement and applicable law.

© The Author(s), under exclusive licence to Springer Nature Limited 2024

## Methods

### Materials

Monomers of AA, HEA, HEMA, acrylamide (AAm) and *N,N*-dimethylacrylamide (DMAAm); butyl acrylate (BA); the covalent crosslinker of MBAA; the ionic liquids of PP, PS, NP and NS; and the photoinitiator of I2959 were purchased from Sigma and used as received without further purification.

### Synthesis of various gels

The glassy gels were fabricated by a one-step polymerization. In a typical procedure, a specified concentration of AA (for example,  $C_m = 6.0$  M), covalent crosslinker of MBAA (0.1 mol%, in a concentration relative to  $C_m$ ) and photoinitiator of I2959 (0.05 mol%, in a concentration relative to  $C_m$ ) were dissolved in PP to form a uniform solution. The solution was then poured into a mould sandwiched between two pieces of glass separated by a spacer and then cured under ultraviolet light (Intelliray 400, 60 mW cm<sup>-2</sup>) for 5 min to obtain the glassy gels. The other ionogels and hydrogels were fabricated in the same process by replacing the solvents (that is, ionic liquids or water) or monomers. Note that the glassy PAA polymer was synthesized by curing AA monomer in water without MBAA, followed by drying at 100 °C until its weight was constant. We also noticed that the fracture strain of the PAA polymer was larger than that in the literature, whereas the Young's modulus was smaller and the fracture strength was almost the same<sup>33</sup>. This may be because of a bit of residual monomer or water in the PAA polymer, which would make it softer and more extensible, but the strength is because of the polymer backbone. In Fig. 1a, the length, width and height are 15.0 mm, 1.5 mm and 10.0 mm, respectively, for the glassy polymer and glassy gel, and they are 15 mm, 10 mm and 10 mm, respectively, for the gel. The monomer concentration is 6.0 M for the glassy gel and gel, whereas the liquid content of the glassy polymer, glassy gel and gel are 0 wt%, 58 wt%, and 56 wt%, respectively.

### Transmittance test

Rectangle samples (width = 20 mm, length = 50 mm and thickness = 2 mm) were used to measure the transmittance of various gels using a UV-Vis-NIR spectrometer (PE Lambda 950, Perkin Elmer) with a wavelength range of 400–800 nm.

### Stability test

Disc-shaped gel samples (thickness = 2 mm and diameter = 12 mm) were prepared, and their weight changes over time at room temperature were recorded. To achieve adequate precision, three samples were measured.

### Mechanical measurements

Tensile properties were measured using a tensile-compressive tester (Instron 5943) at a deformation rate of 100 mm min<sup>-1</sup>. For recovery testing, the sample was first loaded to a certain strain and then unloaded to zero force at a constant velocity of 100 mm min<sup>-1</sup>. The sample was then stored at 80 °C for 1 min to recover. After cooling the sample to room temperature, its tensile stress-strain curve was recorded. The mechanical stability was measured by storing the samples under vacuum at 80 °C, and the tensile stress-strain curves (deformation rate = 100 mm min<sup>-1</sup>) at room temperature were recorded for different durations. Dog-bone-shaped samples with a length of 35 mm, width of 2 mm and gauge length of 12 mm were used in the tensile, recovery and mechanical stability tests. The fracture strength and fracture strain were obtained from the failure point of the tensile stress-strain curve. For gels with a yield point, their modulus was determined by the slope of the linear elastic region (generally ≤5% strain). For gels without a yield point, their modulus was determined from the slope of the first 10% strain of the stress-strain curve.

### NMR test

<sup>13</sup>C NMR spectra of various monomers, ionic liquids and their mixtures in CDCl<sub>3</sub> were recorded using Bruker Avance III 700 MHz NMR.

### Adhesion test

The 90° peeling test was used to evaluate the adhesive properties of the PAA-PP glassy gels. The peeling rate is 50 mm min<sup>-1</sup>. The peeling test samples were prepared with 60 mm length, 19 mm width and 1 mm thickness. The adhesion strength was calculated as the peeling force per width of the gel sheet.

### Conductivity test

The resistance of the glassy gel was measured by the four-point method. The conductivity was calculated as  $\sigma = l/Rs$ , where  $l$ ,  $s$  and  $R$  are the length, cross-sectional area and resistance of the glassy gel, respectively.

### Monomer conversion measurement

To measure the conversion, we extracted the unreacted monomer. Specifically, PAA-PP gels were swollen in a large amount of deionized water for 3 days (requiring a water change every 8 h) to extract unreacted monomers and ionic liquids. Then, the swollen gels were vacuum-dried at 80 °C for 48 h. Therefore, the monomer conversion ( $r$ ) of AA monomer is approximated according to the equation:  $r = m_{\text{PAA}}/m_{\text{AA}}$ , where  $m_{\text{PAA}}$  and  $m_{\text{AA}}$  are the mass of PAA and the mass of AA in the gels, respectively. It should be noted that the PAA-PP-4.0 M gel swelled too much to change the water, so the unreacted monomer was measured instead. Specifically, the PAA-PP-4.0 M gels were soaked in a large amount of deionized water and fully swollen and then vacuum-dried at 80 °C for 48 h. The unreacted AA monomer evaporates during drying, leaving the PAA polymer and ionic liquid. The monomer conversion of the PAA-PP-4.0 M gel is calculated as  $r = (m_{\text{AA}} - m_{\text{unreacted AA}})/m_{\text{AA}}$ , where  $m_{\text{AA}}$  and  $m_{\text{unreacted AA}}$  are the mass of AA and mass of unreacted AA in the gels, respectively.

### SEM imaging

The gel morphologies were characterized by scanning electron microscopy (SEM) (FEI Verios 460 L) at an operating voltage of 2 kV. To observe the morphology, the gels were measured in situ, that is, the ionic liquid solvent in the polymer network was not removed. The gel samples were frozen in liquid nitrogen and then broken by hand to observe their cross-section. A 10-nm layer of gold was coated onto all samples before the SEM analysis.

### Dynamic mechanical analysis

The temperature dependence of the loss tangent ( $\tan \delta$ ) of various gels was measured using a dynamic mechanical analyser (DMA 850, TA Instruments). All the temperature scans were run at 1 Hz frequency at an oscillating strain of 0.1%. The temperature range was -100 °C to 150 °C. A temperature ramp of 3 °C min<sup>-1</sup> was used, and the peak in the  $\tan \delta$  curve was used to define the glass transition temperature ( $T_g$ ).

### FTIR test

The chemical structures of various materials were analysed using FTIR spectroscopy (Spectrum Two FT-IR Spectrometer, Perkin Elmer). All spectra were measured in transmission mode, with data recorded in the range of 4,000–800 cm<sup>-1</sup> over 16 scans.

### Swelling measurements

The swelling performance of various gels were studied by recording the swelling ratios, that is,  $Q_v$  and  $Q_w$ .  $Q_v$  was defined as the ratio of the sample volume at a specific duration,  $V$ , to that of the solution state,  $V_0$ .  $Q_v = V/V_0$ . Similarly,  $Q_w$  was defined as the ratio of the sample weight

# Article

at a specific duration,  $W$ , to that of the solution state,  $W_0$ ,  $Q_w = W/W_0$ . To achieve adequate precision, three samples were measured.

## Joule heating test

Joule heating was demonstrated by a sample consisting of liquid metals sandwiched by two pieces of gels. A current of 3 A was applied to the sample through a DC power supply (SPS3010, Nice-Power), and the sample temperature was recorded in real time using an infrared camera (FLIR SC300-series).

## Data availability

Data generated or analysed during this study are provided as Source data or included in the Supplementary Information. Further data are available from the corresponding author on request. More details on the methods are available in the Supplementary Information. Source data are provided with this paper.

**Acknowledgements** M.D.D. acknowledges support from the Coastal Studies Institute. We thank G. McKenna, Z. Bao, M. Balik and C. Bowman for their helpful discussions. S.S. and B.T.O. acknowledge support from NSF award no. 2324190. W.Q. is partially supported by Nebraska Research Initiative. All NMR measurements were made in the Molecular Education, Technology and Research Innovation Center (METRIC) at NC State University.

**Author contributions** M.W., X.X. and M.D.D. conceived the idea. M.D.D. supervised the project. M.W. carried out most of the experiments. X.X. contributed to the SEM, transmittance test, adhesive demonstration and three-arm gripper design. X.X. and W.B. contributed to the FTIR measurement. S.S. and B.T.O. contributed to the dynamic mechanical analysis test. M.S. participated in the SEM measurement. E.F. participated in the Joule heating measurement. W.Q. contributed to the FTIR analysis. M.W., X.X. and M.D.D. wrote the paper, and all authors reviewed the paper.

**Competing interests** The authors declare no competing interests.

## Additional information

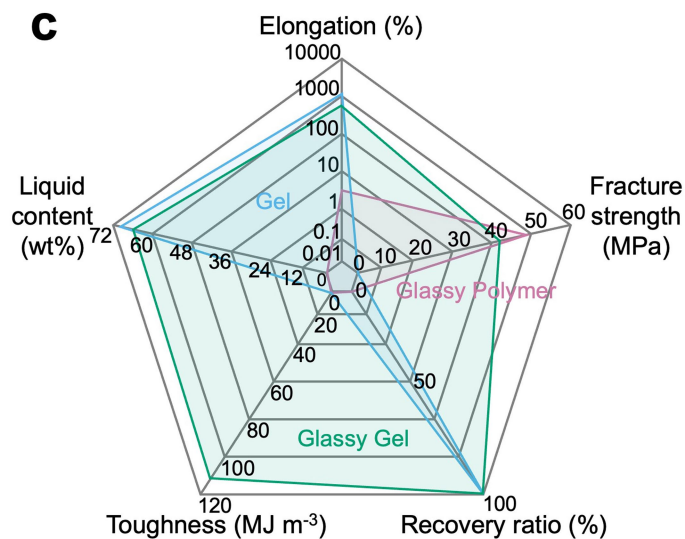
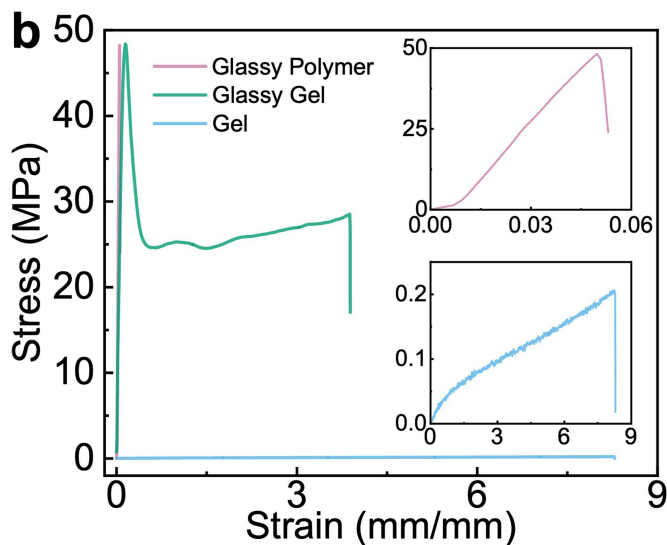
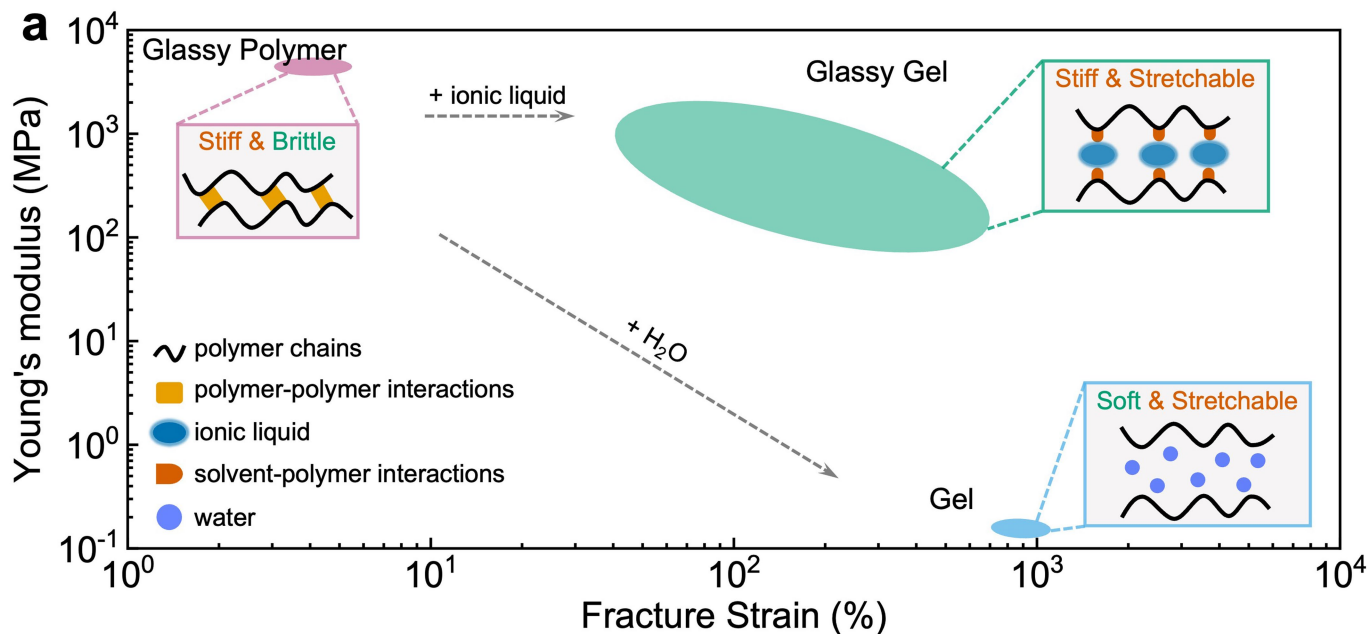
**Supplementary information** The online version contains supplementary material available at <https://doi.org/10.1038/s41586-024-07564-0>.

**Correspondence and requests for materials** should be addressed to Michael D. Dickey.

**Peer review information** Nature thanks Jinhwan Yoon and the other, anonymous, reviewer(s) for their contribution to the peer review of this work.

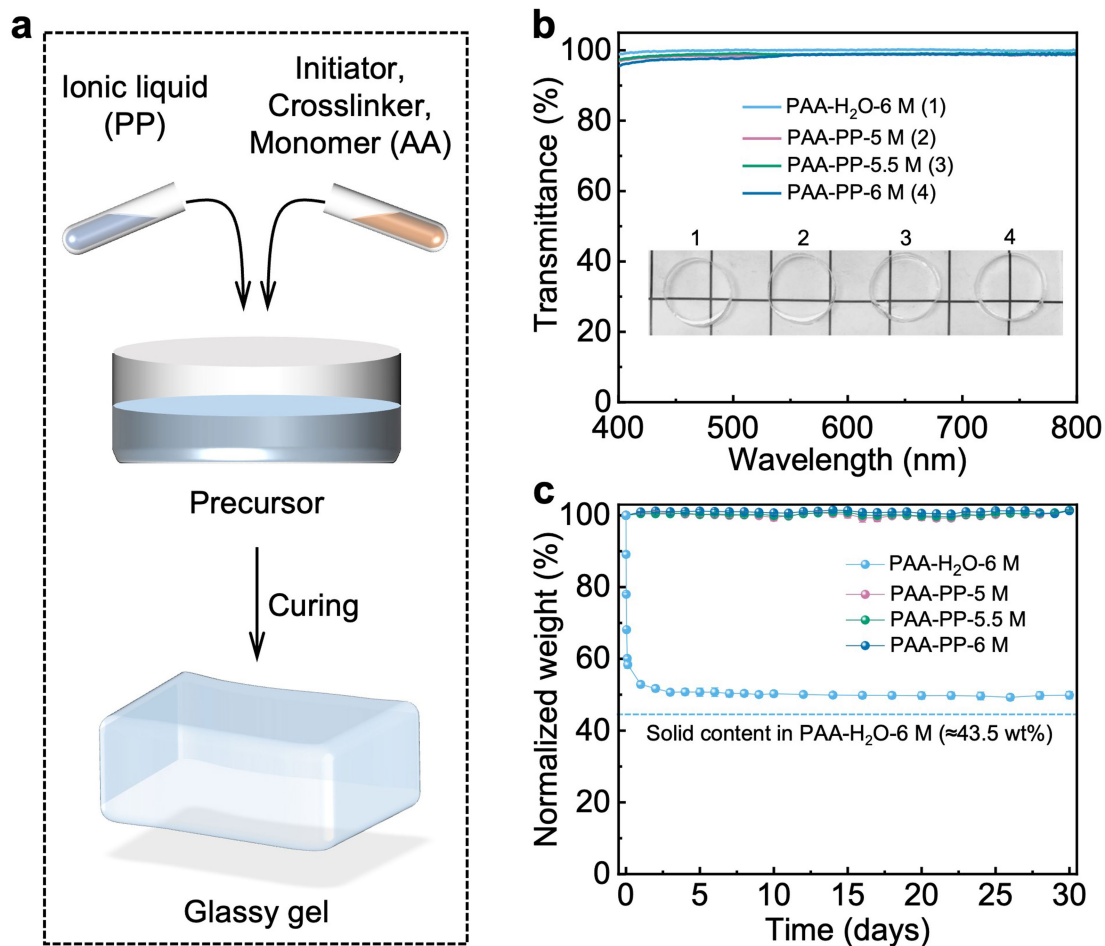
**Reprints and permissions information** is available at <http://www.nature.com/reprints>.





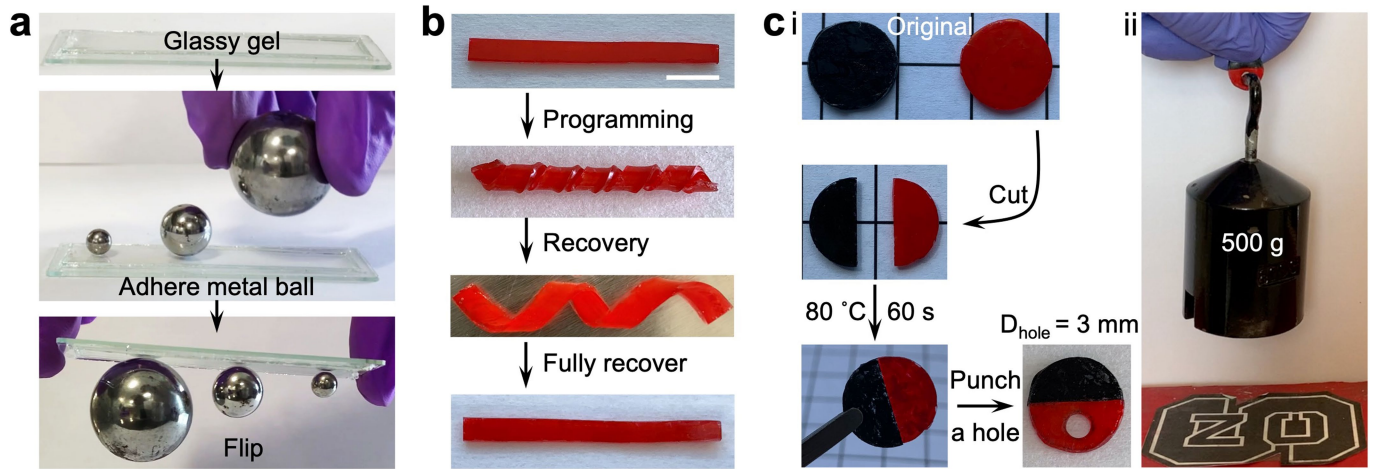
**Extended Data Fig. 1 | Comparison of three classes of polymeric materials.** **a,b**, Schematics (**a**) and tensile stress-strain curves (**b**) illustrating the role of identical solvent loading in gel and glassy gel. Adding solvent improves extensibility of glassy polymers, but usually weakens the mechanical properties (for example, hydrogel). In contrast, glassy gel is extensible like a gel, but stiff like the glassy polymer due to strong solvent-polymer interactions that non-covalently crosslink the polymer. Insets in **b** show individual tensile stress-strain curves. As an example, consider poly(acrylic acid) (PAA). In the absence

of solvent, the polymer is glassy and stiff, yet brittle. Swelling in water produces a hydrogel (56 wt% water) that is many orders of magnitude softer, weaker, and extensible than the glassy polymer. In contrast, replacing water with an ionic liquid solvent (58 wt% ionic liquid) is nearly as stiff as a glass, while maintaining extensibility of a gel. **c**, A spider plot summary in terms of liquid content, toughness, recovery, fracture strength, and elongation. The experimental data is for PAA and the values in **a** are from tensile tests reported in **b, c**, and Supplementary Fig. 4.



**Extended Data Fig. 2 | Synthesis and properties of glassy gels.** **a**, Schematic illustration of the simple one-step approach to synthesize glassy gels from representative monomer (AA) and ionic liquid (PP). **b,c**, Transmission (**b**) and

weight (**c**) changes of various gels. Inset in **b** shows photographs of various gels (thickness = 2 mm, diameter = 12 mm). Error bars on the data in **c** show standard deviation from three independent samples.



**Extended Data Fig. 3 | Glassy gels have multiple functions.** **a**, The ionic bonds give strong adhesion to surfaces despite being stiff and glassy (Middle: metal ball diameter from left to right: 0.25 inch, 0.5 inch and 1 inch). **b**, Heating-induced shape memory (width = 4 mm, length = 4.7 cm). The scale bar is 10 mm.

**c**, Self-healing behavior. The gels merge together after heating at 80 °C for 60 s and are able to support a 500 g hanging weight. The diameter of the gel and the hole is 12 and 3 mm, respectively. In **a-c**, PAA-PP-6.0 M glass gel with a thickness of 1 mm is used.